Published in final edited form as:
*Free Radic Biol Med*. 2014 March ; 68: 8–21. doi:10.1016/j.freeradbiomed.2013.11.007.

# Hypoxia-inducible factor 1 contributes to *N*-acetylcysteine's protection in stroke

**Ziyan Zhang**[a], **Jingqi Yan**[a], **Saeid Taheri**[b], **Ke Jian Liu**[c], and **Honglian Shi**[a,*]

[a]Department of Pharmacology & Toxicology, University of Kansas, Lawrence, KS 66045, USA

[b]Department of Radiology, Medical University of South Carolina, Charleston, SC 29401, USA

[c]Department of Pharmaceutical Sciences, University of New Mexico, Albuquerque, NM 87131, USA

## Abstract

Stroke is a leading cause of adult morbidity and mortality with very limited treatment options. Evidence from preclinical models of ischemic stroke has demonstrated that the antioxidant *N*-acetylcysteine (NAC) effectively protects the brain from ischemic injury. Here, we evaluated a new pathway through which NAC exerted its neuroprotection in a transient cerebral ischemia animal model. Our results demonstrated that pretreatment with NAC increased protein levels of hypoxia-inducible factor-1α (HIF-1α), the regulatable subunit of HIF-1, and its target proteins erythropoietin (EPO) and glucose transporter (GLUT)-3, in the ipsilateral hemispheres of rodents subjected to 90 min middle cerebral artery occlusion (MCAO) and 24 h reperfusion. Interestingly, after NAC pretreatment and stroke, the contralateral hemisphere also demonstrated increased levels of HIF-1α, EPO, and GLUT-3, but to a lesser extent. Suppressing HIF-1 activity with two widely used pharmacological inhibitors, YC-1 and 2ME2, and specific knockout of neuronal HIF-1α abolished NAC's neuroprotective effects. The results also showed that YC-1 and 2ME2 massively enlarged infarcts, indicating that their toxic effect was larger than just abolishing NAC's neuroprotective effects. Furthermore, we determined the mechanism of NAC-mediated HIF-1α induction. We observed that NAC pretreatment upregulated heat-shock protein 90 (Hsp90) expression and increased the interaction of Hsp90 with HIF-1α in ischemic brains. The enhanced association of Hsp90 with HIF-1α increased HIF-1α stability. Moreover, Hsp90 inhibition attenuated NAC-induced HIF-1α protein accumulation and diminished NAC-induced neuroprotection in the MCAO model. These results strongly indicate that HIF-1 plays an important role in NAC-mediated neuroprotection and provide a new molecular mechanism involved in the antioxidant's neuroprotection in ischemic stroke.

### Keywords

HIF-1; Hsp90; NAC; Neuroprotection; Stroke; Free radicals

Stroke is a leading cause of death in the United States and worldwide [1,2]. Reduced supply of oxygen and nutrients results in devastating loss of neurons and leads to defects in brain function in stroke patients [3]. Developing stroke therapeutics remains one of the major



*Corresponding author. Fax: (785) 864 5219. hshi@ku.edu (H. Shi)..

Appendix A. Supporting information

Supplementary data associated with this article can be found in the online version at http://dx.doi.org/10.1016/j.freeradbiomed.2013.11.007.

challenges in clinical medicine. A further exploration of the mechanism of drug candidates in stroke is crucial to the design and implementation of human trials.

Pharmacological effects of *N*-acetylcysteine (NAC) have been studied in stroke models by several research groups. Rodents treated with NAC before ischemia showed reduction in brain infarct volume [4,5], reduced neuronal cell death [6-8], and improvement in neurological function [4]. In addition, NAC is protective in other organs subjected to ischemia, such as heart, liver, lung, and kidney [9-13], and is beneficial in other types of brain diseases such as Parkinson disease [14], Alzheimer disease [15], and amyotrophic lateral sclerosis [16], by slowing down aging and increasing life span [17].

The neuroprotective effects of NAC in ischemia have generally been accredited to its ability to reduce reactive oxygen species (ROS) levels and to inhibit oxidation of lipids, proteins, and DNA. Over the past decades, research progress in cellular redox signaling suggests that antioxidants may exert their biological functions through specific signaling pathways. Studies on pathways that contribute to NAC's neuroprotective effects in ischemia are scarce, although NAC has been suggested to mediate cell survival signaling pathways in other pathological conditions, including cardiovascular, respiratory, and hepatic diseases (see review [18] for detailed discussion). One study has suggested that the neuroprotection of NAC is related to its anti-inflammatory activity through suppression of the activity of nuclear factor-κB (NF-κB) [19]. However, it has been reported that NAC's protective effect is retained even when administered after the NF-κB activation burst [20]. This observation suggested that anti-inflammation might not critically contribute to NAC's neuroprotection. A greater understanding of NAC-mediated changes in key pathways in pathological conditions such as ischemia may provide insights for developing promising therapeutic approaches.

Hypoxia-inducible factor-1 (HIF-1) is a predominant mediator of adaptive responses to decreased oxygen availability, a characteristic of ischemic stroke. HIF-1 is a heterodimer of two subunits, the regulatable HIF-1α and the constitutively expressed and stable HIF-1β [21]. The activity of HIF-1 is primarily determined by the level of its α subunit [22,23]. Our previous study demonstrated that NAC is able to induce HIF-1α expression in primary cortical neurons exposed to hypoxia [24]. Our present study provides experimental evidence that NAC stabilizes HIF-1α and increases its downstream target genes expression in the brains of transient cerebral ischemia animal models. More importantly, we demonstrate for the first time that the protective effects of NAC against ischemic injury were abolished when HIF-1 activity was inhibited by either pharmacological inhibitors or genetic depletion. Furthermore, we reveal a novel mechanism by which NAC upregulates HIF-1α protein expression in ischemic brains.

## Materials and methods

### Animals

All procedures using animals were approved by the Institutional Animal Care and Use Committees of the University of Kansas and the University of New Mexico and conformed to the National Institutes of Health guidelines for use of animals in research. Animals were maintained in a climate-controlled vivarium with a 12-h light-dark cycle with free access to food and water. Male Sprague-Dawley rats, 280-310 g, were from Charles River Laboratory (Wilmington, MA, USA). Mice (B6.129-hif-1α$^{tm3Rsjo}$/J) carrying homozygous HIF-1α floxed alleles (HIF-1α$^{F/F}$) were generated by engineering loxP sites flanking exon 2 of the HIF-1α gene as described previously [25] and were bought from The Jackson Laboratory (Stock No. 007561, Bar Harbor, ME, USA). Mice (B6. Cg-Tg (CaMk2a-cre) T29-1Stl/J) expressing Cre recombinase under the control of the calcium/calmodulin-dependent kinase

(CaMKII) promoter were generated as described previously [26] and also bought from The Jackson Laboratory (Stock No. 005359). All mouse strains were maintained on a C57BL/6 J background. All animals were acclimated to the environment for 7 days before the experiments. The mouse strain B6.Cg-Tg (CaMk2a-cre) was crossed with homozygous HIF-1$\alpha^{F/F}$ mice to generate Cre$^{+/-}$:HIF-1$\alpha^{F/Wt}$, which were crossed with homozygous HIF-1$\alpha^{F/F}$ mice to generate HIF-1α mutants Cre$^{+/-}$:HIF-1$\alpha^{F/F}$, designated as neuron-specific HIF-1α-knockout HIF-1$\alpha^{\Delta/\Delta}$ as described previously [27]. Littermates with the Cre$^{-/-}$:HIF-1$\alpha^{F/F}$ genotype were used as controls for each group of experiments.

## Genotyping

Genomic DNA was isolated from tail biopsies collected at 21 days of age using the DNeasy genomic DNA isolation kit (Qiagen, Valencia, CA, USA). HIF-1$\alpha^{F}$ and wild-type alleles were detected using the following primers: 5′-CGTGTGAGAAAACTTCTGGATG-3′ and 5′-AAAAGTATTGTGTTGGGGCAGT-3′. Transgenic mice expressing Cre recombinase were identified using primers 5′-GCGGTCTGGCAGTAAAAACTATC-3′ and 5′-GTGAAACAGCATTGCTGTCACTT-3′. PCR was performed with the Omni Clenttaq polymerase (DNA Polymerase Co., St. Louis, MO, USA). The products were run on a 3% agarose gel for HIF-1α or Cre. A representative genotype analysis of nine littermates is shown in Supplementary Fig. S1.

## Middle cerebral artery occlusion (MCAO)

For the surgical procedures on rats, 4.0% isoflurane in $N_2O$:$O_2$ (70%:30%) was used for anesthesia induction and 2.0% for anesthesia maintenance. Duration of anesthetic exposure was kept the same for each animal. MCAO followed by reperfusion was conducted using an intraluminal model as previously described [28]. Briefly, the external carotid artery (ECA), internal carotid artery (ICA), and pterygopalatine artery of the ICA were exposed. A silicone rubber-coated monofilament nylon suture (Doccol Corp., Sharon, MA, USA) with a diameter of 0.37 mm was inserted into the ICA via a slit in the ECA. The suture was advanced along the ICA to the extent of 18 to 19 mm from the bifurcation of the rat. Reperfusion was produced by gently withdrawing the suture until the suture tip reached the bifurcation and the incision closed 90 min after the onset of ischemia. After surgery, the animals were allowed to recover from anesthesia while being given food and water ad libitum. Buprenorphine was administered at 0.1 mg/kg subcutaneously as postoperative analgesia. For mouse anesthesia, 2.0% isoflurane in $N_2O$:$O_2$ (70%:30%) was used for induction and 1.0% for maintenance. A similar surgical procedure was performed on mice using smaller-sized sutures, with a diameter of 0.23 mm (Doccol Corp.). The suture was advanced along the ICA to the extent of 9 to 10 mm from the bifurcation of the mouse. For all animals used in this study, successful MCAO was confirmed by laser Doppler flowmetry (LDF; Moor Instruments, Wilmington, DE, USA) as described in the literature [29]. During ischemia, LDF regional cerebral blood flow dropped to 16.9±3.6 (mice) or 15.4±1.8% (rats) of the preischemic level; and after reperfusion the blood flow was restored to 87.6±4.7 (mice) or 90.5±3.6% (rats) of the preischemic level. In addition, the animals were placed on a heating pad during surgery. Body temperature was monitored throughout the surgery process. There was no significant difference in body temperature, which was in the range of 37.0±0.3 °C. Animals that did not show any neurological deficits or had intracranial bleeding during the surgical process were excluded.

## Experimental groups

Sprague-Dawley male rats were randomly assigned to the following nine groups: (1) 3-(5′-hydroxymethyl-2′-furyl)-1-benzylindazole (YC-1) (without MCAO, *n*=5); (2) NAC (without MCAO, *n*=5); (3) 2-methoxyestradiol (2ME2) (without MCAO, *n*=5); (4) MCAO (*n*=25);

(5) MCAO pretreated with NAC (*n*=25); MCAO pretreated (6) MCAO pretreated with YC-1 (*n*=30); (7) with YC-1+NAC (*n*=30); (8) MCAO pretreated with 2ME2 (*n*=30); and (9) MCAO pretreated with 2ME2+NAC (*n*=30). In all the six groups subjected to MCAO, five rats were used for Western blotting of whole contralateral and ipsilateral hemispheres, five rats were used for Western blotting of peri-infarct tissue, five rats were used for immunostaining, and five to eight rats were used for infarct size measurement by magnetic resonance imaging (MRI) and 2,3,5-triphenyltetrazolium chloride (TTC) staining (Table 1). NAC (A7250; Sigma, St. Louis, MO, USA) dissolved in saline with 1% dimethyl sulfoxide (DMSO) was administered at 150 mg/kg body wt intraperitoneally (ip) at 30 min before the onset of ischemia according to a previous publication [8]. Growing evidence suggests that YC-1 and 2ME2 exert an inhibitory effect on the accumulation of HIF-1α induced by hypoxia, iron chelation, and proteasomal inhibition [30-34]. YC-1 has widely been used as a HIF-1 blocker in research. It has been demonstrated that YC-1 effectively inhibits HIF-1 expression in heart [35], kidney [36], and brain [37]. YC-1 may directly degrade HIF-1α protein by inducing the degradation of the C-terminal of HIF-1α protein [38]. It can also suppress the translation of HIF-1α through the PI3K/Akt/mTOR/4E-BP pathway [39]. YC-1 has been reported to inhibit the expression of HIF-1 downstream genes such as erythropoietin (EPO) and vascular endothelial growth factor [32]. 2ME2 inhibits HIF-1α protein synthesis by disrupting microtubules [40]. Both YC-1 and 2ME2 were used as complementary approaches to knockout in determining the effect of HIF-1. YC-1 (Cayman Chemical Co., Ann Arbor, MI, USA) and 2ME2 (Enzo Life Science, Farmingdale, NY, USA) were both dissolved in a solution of 1% DMSO in saline. YC-1 was administered at 2 mg/kg body wt through the femoral vein at 24 h and 30 min before the onset of ischemia. 2ME2 was administered at 5 mg/kg body wt (ip) at 1 h before the onset of ischemia. Rats in the control group received equal-volume injections (ip) of the DMSO solution. We chose the dose of the HIF-1 inhibitors based on previous publications [30,31] and our own analysis of HIF-1α expression.

The HIF-1α knockout (HIF-1α$^{\Delta/\Delta}$) male mice were randomly assigned to two groups: MCAO group (*n*=6) and MCAO pretreated with NAC (*n*=6). Twelve male littermates (HIF-1α$^{F/F}$) were used as controls and randomly assigned to two groups: MCAO group (*n*=6) and MCAO pretreated with NAC (*n*=6). In all four groups, three mice were used for Western blotting analysis and three mice were used for infarct size measurement by TTC. In mouse models of MCAO/reperfusion, NAC was administered at 240 mg/kg (dissolved in saline) body weight (ip) at 30 min before the onset of ischemia. The NAC dose for mice was calculated from the rat dose using body surface area normalization [41]. Mice in control and HIF-1α knockout groups received an equal volume of saline injection (ip).

The effect of 17-allylamino-17-demethoxygeldanamycin (17-AAG; AG Scientific, San Diego, CA, USA) was tested in the following groups of mice: NAC (without MCAO, *n*=3), 17-AAG (without MCAO, *n*=3), MCAO (*n*=3), MCAO pretreated with NAC (*n*=3), MCAO pretreated with 17-AAG (*n*=3), and MCAO pretreated with 17-AAG+NAC (*n*=3). 17-AAG is a derivative of the antibiotic geldanamycin and is widely used as a heat-shock protein 90 (Hsp90) inhibitor. 17-AAG was dissolved in a solution of 1% DMSO in saline and administered at 25 mg/kg (ip) at 1 h before the onset of ischemia. Mice in control and NAC groups received an equal volume of the DMSO solution (ip).

Usually four or five animals were randomly selected for surgery on a given day. A randomized block design was used: within each day, each animal was allocated at random to one of the available treatments. The following final analyses were performed by researchers who were blinded to the treatments and animal groups.

### Western blotting and coimmunoprecipitation (co-IP)

At 24 h reperfusion, the animals were anesthetized and euthanized by decapitation. The ipsilateral and contralateral hemispheres were isolated and homogenized separately for Western blotting assay. We also collected peri-infarct brain tissues and the corresponding region in the contralateral (nonischemic) side. The peri-infarct region was identified using TTC staining in the control MCAO rat model (90 min ischemia and 24 h reperfusion, no pharmacological treatments) as described in our previous publication [42]. Briefly, as marked in Fig. 2A, the ischemic peri-infarct was selected on the one o'clock line in the ipsilateral cortex. Tissues between the dashed lines (about 1.5 mm in width; Fig. 2A) were isolated from the ipsilateral and contralateral hemispheres and homogenized separately for Western blotting. The fixed location, as marked in Fig. 2A, was used for tissue isolation in animals that received different pharmacological treatments. However, the location of peri-infarct varies from animal to animal, especially in animals from different groups. The selected region of treated animals may represent pathological states different from that of the control MCAO rats. Standard Western blotting and co-IP procedures were followed as described previously [30]. The primary antibodies were rabbit anti-HIF-1α (Millipore, Billerica, MA, USA), mouse anti-Hsp90 (SPA-830; Enzo Life Science), rabbit anti-glucose transporter (GLUT-3; ab53095; Abcam, Cambridge, MA, USA), and rabbit anti-EPO (sc-7956; Santa Cruz Biotechnology, Santa Cruz, CA, USA). The secondary antibody for HIF-1α, GLUT-3, and EPO was goat anti-rabbit IgG-horseradish peroxidase (HRP; sc-2030; Santa Cruz Biotechnology). The secondary antibody for Hsp90 was goat anti-mouse IgG-HRP (sc-2030; Santa Cruz Biotechnology). β-Actin was used as an internal control.

### Measurement of infarct size by magnetic resonance imaging and TTC staining

The rats were transported to the MRI room next to the surgery room at 24 h reperfusion and placed in the isocenter of the magnet before the imaging session. MRI was performed on a 4.7-T Biospecs MR scanner (Bruker Biospin, Billerica, MA, USA). An actively shielded gradient coil with a 120-cm inner diameter was used. The animals were kept in the same position throughout imaging. For each animal, we performed T2-weighted MRI by using a rapid acquisition with refocused echo sequence. Image data were then transferred to a workstation running Linux for further processing. From the T2-weighted magnetic resonance images, we calculated the volume of infarction using ImageJ.

After MRI, the brains were removed and sectioned into 2-mm slices. The slices were incubated in a 2% solution of TTC in 0.1 M phosphate-buffered saline (PBS; pH 7.4) at 37 °C for 30 min and fixed in 10% formalin. TTC staining has been widely used to reflect accurately the extent of irreversible ischemic damage in cerebral tissues in rats [43]. TTC-stained brain sections were photographed using a digital camera (Powershot 400 digital camera; Canon). The infarct size was calculated; and the percentage of the infarct area with respect to the total area was digitally quantified by ImageJ. To compensate for the effect of brain edema, the corrected infarct area was calculated as previously described [44].

### Mortality and neurological deficits

Mortality was calculated at 24 h after MCAO/reperfusion. The neurological scores were performed in a blinded fashion at 24 h, based on a modified scoring standard of Rogers et al. [45]. We excluded dead animals in the scoring scale.

### Immunohistochemical staining

After 24 h reperfusion, rats/mice were transcardially perfused with ice-cold PBS under anesthesia and then with 4% paraformaldehyde. After decapitation, the brains were isolated and fixed overnight in 4% paraformaldehyde. The brains were then embedded in OCT

compound (Sakura Finetek USA, Torrance, CA, USA) and sectioned coronally at 10 μm thickness using a vibrating microtome (Leica Microsystems, Bannockburn, IL, USA). Brain sections were washed and the nonspecific binding sites were blocked with PBS containing 0.05% Triton X-100 and 0.25% bovine serum albumin for 1 h. Primary antibodies were diluted in blocking buffer and incubated with sections overnight at 4 °C [30]. Primary antibodies were rabbit anti-HIF-1α (04-1006; Millipore), rabbit anti-GLUT-3 (ab53095; Abcam), rabbit anti-EPO (sc-7956; Santa Cruz), and mouse anti-NeuN (MAB377; Millipore). Secondary antibodies were donkey anti-rabbit Alexa 488 and goat anti-mouse Alexa 488 (Molecular Probes, Carlsbad, CA, USA). The process for selecting the area of interest for imaging was detailed in our previous publication [42]. The imaging location was selected at per-infarct cortex based on TTC staining. As marked in Fig. 2A, the squares indicate the selected area for imaging. Images were routinely captured with a Leica DMI 4000B fluorescence microscope. The original images were converted to 8-bit RBG and the immunoreactivity of each image was analyzed with Image-Pro Plus 5 (Media Cybernetics, Bethesda, MD, USA). Pixel intensity was chosen to reflect changes in protein expression levels in neurons over cell counts. The rationale was that HIF-1α might have been extensively expressed in the neurons in ischemic brain without NAC treatment [27], so the number of the HIF-1α-positive neurons may not be able to reflect further changes in neuronal HIF-1α expression in neurons such as those in the NAC-treated group. The optical density approach is able to reflect further increases in the protein content of HIF-1α-positive neurons. An approximate threshold for pixel intensity was set and applied to images to discriminate positive staining from background signal. Total immunoreactivity was calculated by the area occupied by immunopositive pixels multiplied by the optical density of those pixels. Five consecutive sections per animal were used for analysis. Average values for each animal were used to generate mean values for each treatment. All immunohistochemical staining data were obtained and analyzed in a blinded manner.

### Statistical analysis

Neurological score results are presented as median with range. Other results are presented as mean with a standard error of the mean. Comparisons of Western blotting, immunoreactivity, and infarct volumes were carried out by ANOVA, followed by Tukey's correction (R 3.0.1). Neurological scores were compared using Kruskal-Wallis analysis followed by Bonferroni correction. A $p<0.05$ was considered statistically significant. For the statistical analysis of mortality, the Fisher exact test was used.

## Results

### NAC enhanced global HIF-1α expression in ischemic brains

Previous reports have demonstrated that pretreatment with NAC significantly increased neuronal survival and reduced brain infarct [4,7,8,46]. To investigate the mechanism of NAC's neuroprotective effects during ischemia and reperfusion, NAC was administrated (ip) to rats before the onset of MCAO in this study. Fig. 1 shows Western blotting results of the overall levels of HIF-1α and its downstream proteins in contralateral and ipsilateral hemispheres. Ischemic exposure increased HIF-1α protein expression in the ipsilateral hemisphere, compared to the contralateral one (Figs. 1A and B). NAC further increased HIF-1α expression in the ipsilateral brain tissues. NAC also upregulated the protein expression of EPO and GLUT-3, two downstream factors of HIF-1, in the ipsilateral hemisphere (Figs. 1A-D). The results indicated that NAC effectively enhanced HIF-1α protein accumulation and HIF-1 functional activity in the ischemic brains. In addition, it is of interest to note that NAC also increased the HIF-1α expression in the contralateral side, which is usually used as control in stroke studies. To confirm the effect of NAC on contralateral brain tissue, we also administered NAC to rats that did not receive MCAO

(naïve animals). As shown in Supplementary Fig. S2, NAC promoted HIF-1α expression in the naïve rats' brains.

The above results were obtained using whole-hemisphere homogenates and reflected the effect of NAC on the overall levels of HIF-1α, EPO, and GLUT-3 in both hemispheres. We also determined changes in the protein levels in selected peri-infarct areas as marked in Fig. 2A. Results demonstrated that NAC increased the protein levels of HIF-1α, EPO, and GLUT-3 in the selected region (Supplementary Fig. S3). However, it needs to be pointed out that we isolated the peri-infarct tissue of all the rats from the fixed location that was determined based on control MCAO animals, which received no pharmacological treatments. Because the drug treatments altered the brain infarction, the selected region in the drug-treated animals might represent a pathological state different from that of control rats. We do not exclude the possibility that changes in HIF-1α and its target protein levels might be a result of sampling tissues of different viability. Nevertheless, these results from the selected brain region provide additional insights into the effects of NAC on the expression of HIF-1α, EPO, and GLUT-3 in the ischemic brain.

One of the aims in this study was to determine the role of HIF-1 in NAC-mediated neuroprotection. Inhibiting HIF-1 activity would confirm specifically whether HIF-1 contributes to NAC's effects. YC-1 and 2ME2 are commonly used HIF-1α inhibitors. To inhibit HIF-1, we chose double injections of YC-1 at 2 mg/kg based on our previous report of HIF-1α inhibition [30]. It has been shown that 2ME2 (5 mg/kg. ip) could successfully decrease HIF-1α levels in rat [31]. To successfully inhibit HIF-1α expression in the NAC group, the inhibitors were administered before the injection of NAC. Both inhibitors at the tested doses effectively suppressed HIF-1α, EPO, and GLUT-3 expression in ischemic brains (Figs. 1A-D). It is noteworthy that YC-1 and 2ME2 were able to inhibit HIF-1α expression in the presence of NAC in the contralateral sides (Fig. 1) and in the brains of naïve rats (Supplementary Fig. S2).

### NAC elevated neuronal HIF-1α expression in ischemic brains

As ischemia causes devastating neuronal death in stroke, it was of great interest to determine if NAC enhanced the expression of HIF-1α in neurons. As illustrated in Fig. 2, HIF-1α protein accumulation primarily occurred in the NeuN (neuronal marker)-positive cells in the selected area of the ipsilateral hemispheres. The intensity of HIF-1α immunostaining was further increased in the ipsilateral side of the brains of NAC-treated rats. Moreover, the neuronal expression of EPO and GLUT-3 was significantly increased in the ipsilateral neurons of NAC-treated rats, compared to control rats (Figs. 3A and B, Supplementary Fig. S5). The ipsilateral expression of all three proteins (HIF-1α, EPO, and GLUT-3) was remarkably reduced by the HIF-1α inhibitors, YC-1 and 2ME2, in either NAC-treated or control rats. The above results demonstrate that NAC remarkably enhanced HIF-1α and its downstream genes expression in neurons in the ipsilateral hemisphere of an ischemic brain.

### HIF-1 was responsible for NAC-mediated neuroprotection against ischemic brain injury

To determine the role of HIF-1 in NAC's neuroprotection in ischemic stroke, we first evaluated NAC's protective effects against ischemia/reperfusion-induced brain injury by T2-weighted MRI and TTC staining. Fig. 4A shows a series of brain sections of a rat subjected to 90 min MCAO and 24 h reperfusion. The brain infarct volume was calculated based on the area of hyperintensity of the MR images. As shown in Figs. 4A and B, administration of NAC at 150 mg/kg significantly reduced the infarct volume (140.2±18.8 $mm^3$), compared to the control group (226.0±26.1 $mm^3$; $p$=0.0135). Consistent with the T2-weighted MRI data, the infarct volume measured by TTC-staining also demonstrated that NAC significantly

reduced the brain infarction ($p$=0.0007). These results were in line with previous reports that NAC is neuroprotective in ischemic stroke [4-7,19,47].

Fig. 4 also demonstrated that inhibiting HIF-1α remarkably augmented ischemia-induced brain damage. YC-1 and 2ME2 increased the infarct volume estimated by T2-weighted MRI from 226.0±26.1 to 481.6±27.7 and 477.8±24.1 $mm^3$, respectively ($p$<0.0001). No significant difference was observed among YC-1, YC-1+NAC, 2ME2, and 2ME2+NAC groups, indicating that NAC failed to provide protection against cerebral ischemia in the presence of YC-1 or 2ME2. Results from TTC staining showed similar effects. It is noteworthy that YC-1 and 2ME2 massively enlarged the infarcts, indicating their toxic effect was beyond just abolishing NAC's neuroprotective effects.

We further determined the functional recovery of rats subjected to NAC and HIF-1 inhibitor treatments by behavioral assessment according to Rogers et al. [45]. NAC treatment significantly decreased the median neurological scores from 3 (range 2-4) in control rats to 2 (range 1-3) (control, $n$=22; NAC, $n$=23; $p$=0.0097; Fig. 4D). However, NAC was not able to alleviate neurological abnormalities when HIF-1 activity was inhibited by YC-1 or 2ME2. In addition, two animals were dead in the control group, and one dead was observed in the NAC-treated groups (Table 1). The treatment with NAC, YC-1, or 2ME2 alone did not cause death in negative control animals (without MCAO, data not shown).

## Neuron-specific HIF-1α knockout abolished NAC-mediated neuroprotection in ischemic brains

The above results demonstrate that the pharmacological HIF-1α inhibitors YC-1 and 2ME2 abolished NAC's neuroprotection in the ischemic brains. We further studied the specific role of HIF-1 in NAC-mediated neuroprotection with neuron-specific HIF-1α-knockout mice (HIF-$1\alpha^{\Delta/\Delta}$). CAMKII-dependent Cre expression removed the lox-HIF-1α-lox cassette in the genome of neurons of HIF-$1\alpha^{\Delta/\Delta}$ mice (Fig. 5A). To evaluate the efficiency of HIF-1α ablation in neurons of the HIF-$1\alpha^{\Delta/\Delta}$ mice, we used immunostaining to visualize HIF-1α expression in NeuN-positive cells in the ipsilateral hemisphere of a mouse brain after 90 min MCAO and 24 h reperfusion. HIF-1α expression was diminished in the majority of neurons in HIF-$1\alpha^{\Delta/\Delta}$ mice (Supplementary Fig. S6). Postischemic accumulation of HIF-1α, GLUT-3, and EPO was significantly attenuated in the HIF-$1\alpha^{\Delta/\Delta}$ mice compared with controls (HIF-$1\alpha^{F/F}$; Figs. 5B and C). Moreover, NAC administration failed to increase the expression of HIF-1α and its target genes in ischemic brains of HIF-$1\alpha^{\Delta/\Delta}$ mice. We observed increased infarction in HIF-$1\alpha^{\Delta/\Delta}$ mice compared with wild-type controls (Figs. 5D and E). Pretreatment with NAC significantly reduced the infarct volume in control mice (50% decrease from 63.0±5.6 to 33.3±6.7 $mm^3$, $p$=0.0316), but not in HIF-$1\alpha^{\Delta/\Delta}$ mice (HIF-$1\alpha^{\Delta/\Delta}$, 83.7±7.5 $mm^3$; HIF-$1\alpha^{\Delta/\Delta}$+NAC, 76.3±5.5 $mm^3$, $p$=0.8421). The results further confirmed that NAC's neuroprotective effects were suppressed by HIF-1α inhibition, indicating that HIF-1 is highly involved in NAC's protection against ischemic brain injury. It is noteworthy that, compared to the rat MCAO model with NAC treatment that had infarct mainly in the striatum, the mouse model's damage was restricted largely in the cortex.

## Hsp90 was involved in NAC-mediated HIF-1α upregulation in ischemic brains

We then investigated the mechanism underlying NAC-induced HIF-1α upregulation in ischemic brains. Previous studies have shown that Hsp90 is able to bind and stabilize HIF-1α [48]. We postulated that NAC might increase HIF-1α protein levels by promoting the expression and chaperone activities of Hsp90. We therefore determined the Hsp90 protein level and Hsp90-HIF-1α interaction in NAC-treated MCAO models. As we expected, NAC administration significantly upregulated Hsp90 expression in the ipsilateral hemispheres of MCAO mice (Figs. 6A and D). Meanwhile, NAC also increased the amount

of Hsp90 pulled down by anti-HIF-1α antibody (Figs. 6A and B), indicating that NAC enhanced the association between Hsp90 and HIF-1α. The results strongly supported the concept that NAC-induced HIF-1α upregulation was accompanied by increased Hsp90 expression and strengthened Hsp90-HIF-1α interaction.

To better evaluate the contribution of Hsp90 to NAC-mediated HIF-1α upregulation, we inhibited Hsp90 activity with 17-AAG, which is blood-brain barrier permeative and specifically binds to Hsp90 [49]. As shown in Fig. 6A, 17-AAG remarkably reduced the interaction of Hsp90 with HIF-1α and suppressed HIF-1α protein expression. It completely abolished the HIF-1α upregulation in NAC-treated ischemic mouse brains, suggesting that Hsp90 was involved in NAC-induced HIF-1α accumulation. Furthermore, 17-AAG significantly increased the infarction in control and NAC-treated animals subjected to 90 min MCAO and 24 h reperfusion (Fig. 7). In conclusion, our results suggest that NAC promoted HIF-1α stabilization by increasing Hsp90 protein expression and the Hsp90-HIF-1α interaction.

## Discussion

Many previous studies have demonstrated that NAC protects against cellular injury from various stresses including ischemia. The beneficial effect of NAC has been largely attributed to its antioxidant properties, specifically speaking, to its ability to reduce ROS and lipid peroxidation. In this study, we defined a new mechanism (i.e., upregulating the protein level of HIF-1α) by which NAC exerts its protective effect against ischemic insults.

As an antioxidant, NAC alters the cellular redox environment, which plays a critical role in normal cellular functions. HIF-1α, the unstable subunit of HIF-1, can be strongly regulated by the cellular redox environment. For example, excessive ROS disrupt HIF-1α accumulation such as in HeLa cells [22] and renal medullary interstitial cells [50]. In contrast, antioxidants such as NAC have been reported to stabilize HIF-1α in epithelial cells [51] and in primary culture cortical neurons as demonstrated in our previous study [24]. However, it was not known whether NAC stabilizes HIF-1α in ischemic brain. In line with these observations, this study, for the first time, showed that NAC administration increased the protein expression of HIF-1α and its target genes EPO and GLUT-3 [52] in the ipsilateral side of an ischemic brain. More importantly, HIF-1 inhibition diminished the neuroprotection by NAC, substantiating the involvement of HIF-1 in NAC's protective effects. These results clearly present that upregulating HIF-1 activity is a new function of NAC in ischemic brain.

We also determined the level of HIF-1α protein in a specific region of an ischemic brain, the peri-infarct region defined in control MCAO rats (90 min ischemia and 24 h reperfusion). The peri-infarct region is at risk for delayed neuronal death owing to the deleterious metabolic processes propagated from the ischemic core to the neighboring tissue, including excitotoxicity, oxidative stress, and inflammation [53]. The surviving neurons in the peri-infarct region directly contribute to behavioral recovery after stroke [54,55]. Previous studies have demonstrated that HIF-1α induction reduced cell death of neurons located in the peri-infarct region [56]. Thus, the peri-infarct tissue is a crucial neuroprotection target, and it is ideal to define how NAC alters HIF-1α expression in this region. Our results showed that NAC upregulated the protein levels of HIF-1α, GLUT-3, and EPO in the peri-infarct brain region. However, results from the selected peri-infarct brain tissue have limitations. The fixed brain region was identified based on control MCAO animals. We isolated the samples from the same location as peri-infarct in animals that received different treatments. Actually, the location of the peri-infarct area varies between animals, and it moves especially when the treatment induces neuroprotection. As a result, the selected brain

region that represented the peri-infarct region in control MCAO animals did not necessarily represent the peri-infarct region in animals that received different treatments. For example, the selected brain tissue in NAC-treated rats might be more normal (healthier) than that in control rats. The measurement of the protein level in whole-hemisphere homogenates avoided the issue of peri-infarct shifting in the various groups. The Western blotting results of whole hemisphere reflected the effects of NAC on the overall levels of HIF-1α, EPO, and GLUT-3 in whole ischemic hemisphere including infarct core, peri-infarct regions, and nonischemic remote areas. Many previous studies have used whole-hemisphere homogenates to determine protein expression in contra- and ipsilateral sides of ischemic brains [27,57-60]. Our results demonstrated that NAC enhanced HIF-1α expression in the ipsilateral side. It is noteworthy that NAC also enhanced HIF-1α and its target gene expression in the contralateral side, suggesting that NAC's effect on HIF-1α is independent of its neuroprotection. Furthermore, our study showed that NAC failed to reduce the brain infarction in HIF-1α-knockout mice, which indicates that NAC's neuroprotective effect depends on increasing HIF-1α expression. Both aspects of the experimental evidence support that HIF-1α upregulation is the mediator of NAC's neuroprotection, rather than the consequence.

Although it is known that redox regulates HIF-1α expression in many cells as discussed above, the mechanism responsible for the regulation is far from completely understood. Hsp90 is among the most abundant proteins in the cytosol of eukaryotic cells. As chaperone, Hsp90 prevents the aggregation of unfolded proteins induced by stresses such as heat shock and ischemia. It has been shown that Hsp90 interacts with transcription factors with the bHLH-PAS domain, such as Sim and Ahrhr. HIF-1α is a transcription factor containing the bHLH-PAS domain, suggesting that Hsp90 may interact with HIF-1α. In fact, Isaacs et al. [61] have shown that Hsp90 antagonist inhibits HIF-1α expression and reduces its target gene mRNA. Therefore, we postulated that NAC might stabilize HIF-1α by promoting its interaction with Hsp90. Indeed, we found that NAC administration upregulated the Hsp90 protein level by 27.3% and enhanced the interaction between Hsp90 and HIF-1α in the ipsilateral hemisphere of an ischemic brain. Given the fact that Hsp90's chaperoning capacity vastly exceeds the demand for more than 200 client targets under normal conditions [62,63], this moderate increase in Hsp90 protein level and interaction may sufficiently account for the 54% increase in the HIF-1α protein level (Fig. 6). The Hsp90 inhibitor 17-AAG attenuated the interaction between Hsp90 and HIF-1α although it did not reduce Hsp90 protein expression in ischemic brains. The fact that 17-AAG inhibited HIF-1α upregulation in the presence of NAC indicated that Hsp90 activity was required for NAC-induced HIF-1α accumulation. However, the mechanism of NAC-mediated Hsp90 upregulation is not known. Suppressing oxidation or other properties of NAC may contribute to the upregulation, which warrants further investigation.

In this study, we demonstrated that the neuroprotective effect of NAC was largely mediated by HIF-1α induction and HIF-1 activation. Although we have provided data to show that Hsp90 is involved in the stabilization of HIF-1α by NAC, it is not known how exactly NAC promotes the interaction between Hsp90 and HIF-1α and stabilizes HIF-1α. We postulate that NAC, an antioxidant, may do so by maintaining redox homeostasis in ischemic brains. As shown in Supplementary Fig. S4, NAC, which increased the GSH/GSSG ratio, induced significant expression of HIF-1α in peri-infarct. L-Buthionine sulfoxide (BSO), which decreased the GSH/GSSG ratio, decreased HIF-1α expression in the peri-infarct. Moreover, NAC increased HIF-1α expression in the contralateral side (Fig. 1 and Supplementary Fig. S4) as well as in the brain of naïve animals (Supplementary Fig. S2). BSO decreased the level of HIF-1α in the contralateral side although no significance was observed owing to low basal levels of HIF-1α in normal brain tissue. The opposite effects of NAC and BSO indicate that NAC might upregulate HIF-1α by reducing oxidants. These results are in line

with our previous observation on primary cultured neurons [24]. In the previous studies, we investigated the relationships between HIF-1α expression, ROS, and redox status in neurons. We observed low levels of HIF-1α protein expression in the neurons exposed to in vitro ischemic conditions that had high levels of ROS (oxidizing environments), and vice versa. NAC induced HIF-1α protein expression in hypoxic neurons and BSO inhibited the expression. Moreover, (−)-epicatechin gallate, an ROS scavenger, elevated HIF-1α expression in the neurons subjected to in vitro ischemia. Taken together, these data indicate that NAC may promote HIF-1α stabilization by suppressing ROS and maintaining cellular redox homeostasis. Evaluation on oxidative stress levels in the experimental groups and effects of other antioxidants on HIF-1 would provide more evidence for the concept, which needs to be investigated in future studies.

There were several considerations for using YC-1 and 2ME2 in this study. First, the two compounds are the most specific inhibitors available. Second, they have been widely used to inhibit HIF-1 activity [31-41]. Third, as in previous publications, they provided effective HIF-1 inhibition. Fourth, they were included in this study to complement the HIF-1α-knockout model. The results demonstrated that the effects of these drugs were enormous on infarct volume, indicating they may act on other pathways that exacerbate brain injury after MCAO. The effects of YC-1 and 2ME2 were so enormous that the effects of NAC were completely saturated by the HIF-1 inhibitors. These are novel findings regarding the two commonly used HIF-1 inhibitors in ischemic brain. To some extent, the effects of the two HIF-1 inhibitors provided evidence to support the concept that NAC lost its protective effect in the MCAO models in the presence of either of the two drugs although other unidentified pathways were obviously involved. In addition, we found that genetic inactivation of HIF-1α resulted in lower infarct volume augmentation than pharmacological inhibition of HIF-1α (Figs. 4A and 5D). This might be due to the activation of compensatory pathways in response to HIF-1α deletion and alteration of non-HIF-1 pathways by the inhibitors. For example, a previous study reported higher basal protein level of HIF-2α and an enhanced upregulation of HIF-2α under hypoxia in HIF-1α-knockout brains [27]. The upregulation of HIF-2α may partially substitute for the loss of HIF-1α function and participate in neuroprotection in the ischemic brain. YC-1 and 2ME2 are able to downregulate the α subunit of both HIF-1 and HIF-2 [40,64], and as the result, they augment infarct volume further than the HIF-1α gene inactivation approach. Overall, the data obtained from knockout mice are evident that NAC mediates its neuroprotection by regulating HIF-1 activity with support from the results of YC-1 and 2ME2.

HIF-1's role in cerebral ischemia is still arguable. Accumulating evidence shows that induction of HIF-1 provides protection against cerebral ischemic damage in adult animals [56,65,66] as well as neonatal models [67]. The protective function of HIF-1 mainly results from a broad range of genes that HIF-1 regulates. The gene expression facilitates the adaptation to low-oxygen conditions [68]. As demonstrated in this study, enhanced expression of HIF-1 by NAC induced the expression of EPO and GLUT-3, which facilitate cell survival and oxygen and glucose transport. However, others have reported detrimental effects of HIF-1 in models of hypoxia and cerebral ischemia [69-71]. The discrepancy of these observations may be partly explained by distinctive effects of HIF-1 at different severities of ischemia. For example, HIF-1 is neuroprotective in a 30-min transient MCAO model [27], whereas it is harmful in a 75-min model of bilateral common carotid artery occlusion [69]. Given the effect of NAC on HIF-1 expression, NAC (or other antioxidants) may have different effects on neurons under different ischemic conditions. Future studies on this aspect may help design therapeutic approaches for specific conditions of ischemia.

In the translational aspect, this study provides novel insight into the mechanism of NAC's prophylactic effect on ischemic brain injury. NAC is a commercially available supplement.

It is of interest to know its effects when taken prophylactically. The pretreatment dose of NAC used in this study is comparable to those of previous studies. For example, Niu et al. [7] reported that pretreatment with NAC at 150 mg/kg could prevent death-associated protein from trafficking and increase the number of the surviving CA1 pyramidal cells of the hippocampus at 5 days of reperfusion. Pretreatment with NAC 30 min before transient forebrain ischemia successfully increased the neuronal survival in rats [8]. Results by Zhang et al. [46] showed that at a dose of 100 mg/kg, pretreatment with NAC distinctly inhibited the association of postsynaptic density protein 95 with kainate receptor glutamate receptor 6 and ameliorated brain injury induced by ischemia. Sekhon et al. [4] reported that animals pretreated with NAC at 150 mg/kg showed a 49.7% reduction in brain infarct volume and 50% reduction in the neurological evaluation score compared to untreated animals. Meanwhile, post-treatment with NAC has also been shown to be neuroprotective in ischemic brains at a similar dose range [5,19,72]. For instance, a single dose of NAC given 15 min after trauma might be effective on lipid peroxidation, antioxidant enzyme activity, and neuronal protection in cerebral injury after closed head trauma [72]. However, the present study using pretreatment only has its limitations and caveats and provides no direct evidence to reveal the mechanism of NAC's neuroprotective effect in postinjury treatment. It is of interest and clinically relevant in future studies to determine the possible mechanism of neuroprotection by NAC treatment after the occurrence of ischemia.

In summary, our data provide evidence that pretreatment with NAC upregulates HIF-1 activity in ischemic brains and demonstrate for the first time that NAC-induced neuroprotection against ischemia is dependent on HIF-1 activity. Moreover, the results reveal a new pathway through which NAC augments HIF-1 activity by enhancing Hsp90 expression and Hsp90-HIF-1α interaction. Our study suggests a new mechanism through which NAC protects stroke-induced brain injury, which may further improve the chances of identifying promising therapeutic approaches in future studies.

## Supplementary Material

Refer to Web version on PubMed Central for supplementary material.

## Acknowledgments

We are indebted to Dr. Bo Zhou for performing surgery on some rat MCAO models. This research was supported in part by a grant from the National Institutes of Health (R01NS058807) and a Kansas University Center for Research startup fund.

## References

[1]. Shuaib A, Hussain MS. The past and future of neuroprotection in cerebral ischaemic stroke. Eur. Neurol. 2008; 59:4–14. [PubMed: 17917451]

[2]. Kung HC, Hoyert DL, Xu J, Murphy SL. Deaths: final data for 2005. Natl. Vital Stat. Rep. 2008; 56:1–120. [PubMed: 18512336]

[3]. Yuan J. Neuroprotective strategies targeting apoptotic and necrotic cell death for stroke. Apoptosis. 2009; 14:469–477. [PubMed: 19137430]

[4]. Sekhon B, Sekhon C, Khan M, Patel SJ, Singh I, Singh AK. N-acetyl cysteine protects against injury in a rat model of focal cerebral ischemia. Brain Res. 2003; 971:1–8. [PubMed: 12691831]

[5]. Wang X, Svedin P, Nie C, Lapatto R, Zhu C, Gustavsson M, Sandberg M, Karlsson JO, Romero R, Hagberg H, Mallard C. N-acetylcysteine reduces lipopolysaccharide-sensitized hypoxic-ischemic brain injury. Ann. Neurol. 2007; 61:263–271. [PubMed: 17253623]

[6]. Cuzzocrea S, Mazzon E, Costantino G, Serraino I, Dugo L, Calabro G, Cucinotta G, De Sarro A, Caputi AP. Beneficial effects of n-acetylcysteine on ischaemic brain injury. Br. J. Pharmacol. 2000; 130:1219–1226. [PubMed: 10903958]

[7]. Niu YL, Li C, Zhang GY. Blocking Daxx trafficking attenuates neuronal cell death following ischemia/reperfusion in rat hippocampus CA1 region. Arch. Biochem. Biophys. 2011; 515:89–98. [PubMed: 21843499]

[8]. Knuckey NW, Palm D, Primiano M, Epstein MH, Johanson CE. N-acetylcysteine enhances hippocampal neuronal survival after transient forebrain ischemia in rats. Stroke. 1995; 26:305–310. [PubMed: 7831704]

[9]. Glantzounis GK, Yang W, Koti RS, Mikhailidis DP, Seifalian AM, Davidson BR. The role of thiols in liver ischemia-reperfusion injury. Curr. Pharm. Des. 2006; 12:2891–2901. [PubMed: 16918419]

[10]. Fischer UM, Cox CS Jr, Allen SJ, Stewart RH, Mehlhorn U, Laine GA. The antioxidant N-acetylcysteine preserves myocardial function and diminishes oxidative stress after cardioplegic arrest. J. Thorac. Cardiovasc. Surg. 2003; 126:1483–1488. [PubMed: 14666023]

[11]. Cakir O, Oruc A, Kaya S, Eren N, Yildiz F, Erdinc L. N-acetylcysteine reduces lung reperfusion injury after deep hypothermia and total circulatory arrest. J. Card. Surg. 2004; 19:221–225. [PubMed: 15151648]

[12]. Sehirli AO, Sener G, Satiroglu H, Ayanoglu-Dulger G. Protective effect of N-acetylcysteine on renal ischemia/reperfusion injury in the rat. J. Nephrol. 2003; 16:75–80. [PubMed: 12653105]

[13]. DiMari J, Megyesi J, Udvarhelyi N, Price P, Davis R, Safirstein R. N-acetyl cysteine ameliorates ischemic renal failure. Am. J. Physiol. 1997; 272:F292–298. [PubMed: 9087670]

[14]. Berman AE, Chan WY, Brennan AM, Reyes RC, Adler BL, Suh SW, Kauppinen TM, Edling Y, Swanson RA. N-acetylcysteine prevents loss of dopaminergic neurons in the EAAC1$^{-/-}$ mouse. Ann. Neurol. 2011; 69:509–520. [PubMed: 21446024]

[15]. Xu J, Chen S, Ku G, Ahmed SH, Chen H, Hsu CY. Amyloid beta peptide-induced cerebral endothelial cell death involves mitochondrial dysfunction and caspase activation. J. Cereb. Blood Flow Metab. 2001; 21:702–710. [PubMed: 11488539]

[16]. Andreassen OA, Dedeoglu A, Klivenyi P, Beal MF, Bush AI. N-acetyl-L-cysteine improves survival and preserves motor performance in an animal model of familial amyotrophic lateral sclerosis. Neuroreport. 2000; 11:2491–2493. [PubMed: 10943709]

[17]. Brack C, Bechter-Thuring E, Labuhn M. N-acetylcysteine slows down ageing and increases the life span of Drosophila melanogaster. Cell. Mol. Life Sci. 1997; 53:960–966. [PubMed: 9447249]

[18]. Zafarullah M, Li WQ, Sylvester J, Ahmad M. Molecular mechanisms of N-acetylcysteine actions. Cell. Mol. Life Sci. 2003; 60:6–20. [PubMed: 12613655]

[19]. Khan M, Sekhon B, Jatana M, Giri S, Gilg AG, Sekhon C, Singh I, Singh AK. Administration of N-acetylcysteine after focal cerebral ischemia protects brain and reduces inflammation in a rat model of experimental stroke. J. Neurosci. Res. 2004; 76:519–527. [PubMed: 15114624]

[20]. Carroll JE, Howard EF, Hess DC, Wakade CG, Chen Q, Cheng C. Nuclear factor-kappa B activation during cerebral reperfusion: effect of attenuation with N-acetylcysteine treatment. Brain Res. Mol. Brain Res. 1998; 56:186–191. [PubMed: 9602121]

[21]. Wang GL, Jiang BH, Rue EA, Semenza GL. Hypoxia-inducible factor 1 is a basic-helix-loop-helix-PAS heterodimer regulated by cellular $O_2$ tension. Proc. Natl. Acad. Sci. USA. 1995; 92:5510–5514. [PubMed: 7539918]

[22]. Huang LE, Arany Z, Livingston DM, Bunn HF. Activation of hypoxia-inducible transcription factor depends primarily upon redox-sensitive stabilization of its alpha subunit. J. Biol. Chem. 1996; 271:32253–32259. [PubMed: 8943284]

[23]. Jiang BH, Rue E, Wang GL, Roe R, Semenza GL. Dimerization, DNA binding, and transactivation properties of hypoxia-inducible factor 1. J. Biol. Chem. 1996; 271:17771–17778. [PubMed: 8663540]

[24]. Guo S, Bragina O, Xu Y, Cao Z, Chen H, Zhou B, Morgan M, Lin Y, Jiang BH, Liu KJ, Shi H. Glucose up-regulates HIF-1 alpha expression in primary cortical neurons in response to hypoxia through maintaining cellular redox status. J. Neurochem. 2008; 105:1849–1860. [PubMed: 18266932]

[25]. Ryan HE, Poloni M, McNulty W, Elson D, Gassmann M, Arbeit JM, Johnson RS. Hypoxia-inducible factor-1α is a positive factor in solid tumor growth. Cancer Res. 2000; 60:4010–4015. [PubMed: 10945599]

[26]. Dragatsis I, Zeitlin S. CaMKIIalpha-Cre transgene expression and recombination patterns in the mouse brain. Genesis. 2000; 26:133–135. [PubMed: 10686608]

[27]. Baranova O, Miranda LF, Pichiule P, Dragatsis I, Johnson RS, Chavez JC. Neuron-specific inactivation of the hypoxia inducible factor 1 alpha increases brain injury in a mouse model of transient focal cerebral ischemia. J. Neurosci. 2007; 27:6320–6332. [PubMed: 17554006]

[28]. Liu S, Shi H, Liu W, Furuichi T, Timmins GS, Liu KJ. Interstitial $pO_2$ in ischemic penumbra and core are differentially affected following transient focal cerebral ischemia in rats. J. Cereb. Blood Flow Metab. 2004; 24:343–349. [PubMed: 15091115]

[29]. Takagi K, Ginsberg MD, Globus MY, Busto R, Dietrich WD. The effect of ritanserin, a 5-HT2 receptor antagonist, on ischemic cerebral blood flow and infarct volume in rat middle cerebral artery occlusion. Stroke. 1994; 25:481–485. [PubMed: 8303760]

[30]. Yan J, Zhou B, Taheri S, Shi H. Differential effects of HIF-1 inhibition by YC-1 on the overall outcome and blood-brain barrier damage in a rat model of ischemic stroke. PLoS One. 2011; 6:e27798. [PubMed: 22110762]

[31]. Xin XY, Pan J, Wang XQ, Ma JF, Ding JQ, Yang GY, Chen SD. 2-Methoxyestradiol attenuates autophagy activation after global ischemia. Can. J. Neurol. Sci. 2011; 38:631–638. [PubMed: 21672704]

[32]. Chun YS, Yeo EJ, Choi E, Teng CM, Bae JM, Kim MS, Park JW. Inhibitory effect of YC-1 on the hypoxic induction of erythropoietin and vascular endothelial growth factor in Hep3B cells. Biochem. Pharmacol. 2001; 61:947–954. [PubMed: 11286986]

[33]. Yeo EJ, Chun YS, Cho YS, Kim J, Lee JC, Kim MS, Park JW. YC-1: a potential anticancer drug targeting hypoxia-inducible factor 1. J. Natl. Cancer Inst. 2003; 95:516–525. [PubMed: 12671019]

[34]. Yeo EJ, Chun YS, Park JW. New anticancer strategies targeting HIF-1. Biochem. Pharmacol. 2004; 68:1061–1069. [PubMed: 15313402]

[35]. Nickel EA, Hsieh CH, Chen JG, Schwacha MG, Chaudry IH. Estrogen suppresses cardiac IL-6 after trauma-hemorrhage via a hypoxia-inducible factor 1α-mediated pathway. Shock. 2009; 31:354–358. [PubMed: 18791496]

[36]. Kimura K, Iwano M, Higgins DF, Yamaguchi Y, Nakatani K, Harada K, Kubo A, Akai Y, Rankin EB, Neilson EG, Haase VH, Saito Y. Stable expression of HIF-1α in tubular epithelial cells promotes interstitial fibrosis. Am. J. Physiol. Renal Physiol. 2008; 295:F1023–1029. [PubMed: 18667485]

[37]. Yeh WL, Lu DY, Lin CJ, Liou HC, Fu WM. Inhibition of hypoxia-induced increase of blood-brain barrier permeability by YC-1 through the antagonism of HIF-1α accumulation and VEGF expression. Mol. Pharmacol. 2007; 72:440–449. [PubMed: 17513385]

[38]. Kim HL, Yeo EJ, Chun YS, Park JW. A domain responsible for HIF-1α degradation by YC-1, a novel anticancer agent. Int. J. Oncol. 2006; 29:255–260. [PubMed: 16773207]

[39]. Sun HL, Liu YN, Huang YT, Pan SL, Huang DY, Guh JH, Lee FY, Kuo SC, Teng CM. YC-1 inhibits HIF-1 expression in prostate cancer cells: contribution of Akt/NF-κB signaling to HIF-1α accumulation during hypoxia. Oncogene. 2007; 26:3941–3951. [PubMed: 17213816]

[40]. Mabjeesh NJ, Escuin D, LaVallee TM, Pribluda VS, Swartz GM, Johnson MS, Willard MT, Zhong H, Simons JW, Giannakakou P. 2ME2 inhibits tumor growth and angiogenesis by disrupting microtubules and dysregulating HIF. Cancer Cell. 2003; 3:363–375. [PubMed: 12726862]

[41]. Reagan-Shaw S, Nihal M, Ahmad N. Dose translation from animal to human studies revisited. FASEB J. 2008; 22:659–661. [PubMed: 17942826]

[42]. Bragin DE, Zhou B, Ramamoorthy P, Muller WS, Connor JA, Shi H. Differential changes of glutathione levels in astrocytes and neurons in ischemic brains by two-photon imaging. J. Cereb. Blood Flow Metab. 2010; 30:734–738. [PubMed: 20104233]

[43]. Bederson JB, Pitts LH, Germano SM, Nishimura MC, Davis RL, Bartkowski HM. Evaluation of 2,3,5-triphenyltetrazolium chloride as a stain for detection and quantification of experimental cerebral infarction in rats. Stroke. 1986; 17:1304–1308. [PubMed: 2433817]

[44]. Schabitz WR, Li F, Irie K, Sandage BW Jr, Locke KW, Fisher M. Synergistic effects of a combination of low-dose basic fibroblast growth factor and citicoline after temporary experimental focal ischemia. Stroke. 1999; 30:427–431. [PubMed: 9933283]

[45]. Rogers DC, Campbell CA, Stretton JL, Mackay KB. Correlation between motor impairment and infarct volume after permanent and transient middle cerebral artery occlusion in the rat. Stroke. 1997; 28:2060–2065. discussion 2066. [PubMed: 9341719]

[46]. Zhang QG, Tian H, Li HC, Zhang GY. Antioxidant N-acetylcysteine inhibits the activation of JNK3 mediated by the GluR6-PSD95-MLK3 signaling module during cerebral ischemia in rat hippocampus. Neurosci. Lett. 2006; 408:159–164. [PubMed: 17030433]

[47]. Lee TF, Tymafichuk CN, Bigam DL, Cheung PY. Effects of postresuscitation N-acetylcysteine on cerebral free radical production and perfusion during reoxygenation of hypoxic newborn piglets. Pediatr. Res. 2008; 64:256–261. [PubMed: 18437097]

[48]. Liu YV, Baek JH, Zhang H, Diez R, Cole RN, Semenza GL. RACK1 competes with HSP90 for binding to HIF-1α and is required for $O_2$-independent and HSP90 inhibitor-induced degradation of HIF-1α. Mol. Cell. 2007; 25:207–217. [PubMed: 17244529]

[49]. Waza M, Adachi H, Katsuno M, Minamiyama M, Sang C, Tanaka F, Inukai A, Doyu M, Sobue G. 17-AAG, an Hsp90 inhibitor, ameliorates polyglutamine-mediated motor neuron degeneration. Nat. Med. 2005; 11:1088–1095. [PubMed: 16155577]

[50]. Yang ZZ, Zhang AY, Yi FX, Li PL, Zou AP. Redox regulation of HIF-1α levels and HO-1 expression in renal medullary interstitial cells. Am. J. Physiol. Renal Physiol. 2003; 284:F1207–1215. [PubMed: 12595275]

[51]. Haddad JJ, Olver RE, Land SC. Antioxidant/pro-oxidant equilibrium regulates HIF-1α and NF-kappa B redox sensitivity: evidence for inhibition by glutathione oxidation in alveolar epithelial cells. J. Biol. Chem. 2000; 275:21130–21139. [PubMed: 10801793]

[52]. Semenza GL. Hypoxia-inducible factor 1: master regulator of $O_2$ homeostasis. Curr. Opin. Genet. Dev. 1998; 8:588–594. [PubMed: 9794818]

[53]. Brown CE, Wong C, Murphy TH. Rapid morphologic plasticity of peri-infarct dendritic spines after focal ischemic stroke. Stroke. 2008; 39:1286–1291. [PubMed: 18323506]

[54]. Cramer SC, Shah R, Juranek J, Crafton KR, Le V. Activity in the peri-infarct rim in relation to recovery from stroke. Stroke. 2006; 37:111–115. [PubMed: 16306462]

[55]. Murphy TH, Corbett D. Plasticity during stroke recovery: from synapse to behaviour. Nat. Rev. Neurosci. 2009; 10:861–872. [PubMed: 19888284]

[56]. Kunze R, Zhou W, Veltkamp R, Wielockx B, Breier G, Marti HH. Neuron-specific prolyl-4-hydroxylase domain 2 knockout reduces brain injury after transient cerebral ischemia. Stroke. 2012; 43:2748–2756. [PubMed: 22933585]

[57]. Althaus J, Bernaudin M, Petit E, Toutain J, Touzani O, Rami A. Expression of the gene encoding the pro-apoptotic BNIP3 protein and stimulation of hypoxia-inducible factor-1α (HIF-1α) protein following focal cerebral ischemia in rats. Neurochem. Int. 2006; 48:687–695. [PubMed: 16464515]

[58]. van den Tweel ER, Kavelaars A, Lombardi MS, Nijboer CH, Groenendaal F, van Bel F, Heijnen CJ. Bilateral molecular changes in a neonatal rat model of unilateral hypoxic-ischemic brain damage. Pediatr. Res. 2006; 59:434–439. [PubMed: 16492985]

[59]. Cipriani R, Villa P, Chece G, Lauro C, Paladini A, Micotti E, Perego C, De Simoni MG, Fredholm BB, Eusebi F, Limatola C. CX3CL1 is neuroprotective in permanent focal cerebral ischemia in rodents. J. Neurosci. 2011; 31:16327–16335. [PubMed: 22072684]

[60]. Singhal AB, Wang X, Sumii T, Mori T, Lo EH. Effects of normobaric hyperoxia in a rat model of focal cerebral ischemia-reperfusion. J. Cereb. Blood Flow Metab. 2002; 22:861–868. [PubMed: 12142571]

[61]. Isaacs JS, Jung YJ, Mimnaugh EG, Martinez A, Cuttitta F, Neckers LM. Hsp90 regulates a von Hippel Lindau-independent hypoxia-inducible factor-1α-degradative pathway. J. Biol. Chem. 2002; 277:29936–29944. [PubMed: 12052835]

[62]. Taipale M, Jarosz DF, Lindquist S. HSP90 at the hub of protein homeostasis: emerging mechanistic insights. Nat. Rev. Mol. Cell Biol. 2010; 11:515–528. [PubMed: 20531426]

[63]. Picard D. Heat-shock protein 90, a chaperone for folding and regulation. Cell. Mol. Life Sci. 2002; 59:1640–1648. [PubMed: 12475174]

[64]. Li SH, Shin DH, Chun YS, Lee MK, Kim MS, Park JW. A novel mode of action of YC-1 in HIF inhibition: stimulation of FIH-dependent p300 dissociation from HIF-1α. Mol. Cancer Ther. 2008; 7:3729–3738. [PubMed: 19074848]

[65]. Ogle ME, Gu X, Espinera AR, Wei L. Inhibition of prolyl hydroxylases by dimethyloxaloylglycine after stroke reduces ischemic brain injury and requires hypoxia inducible factor-1α. Neurobiol. Dis. 2012; 45:733–742. [PubMed: 22061780]

[66]. Karuppagounder SS, Ratan RR. Hypoxia-inducible factor prolyl hydroxylase inhibition: robust new target or another big bust for stroke therapeutics? J. Cereb. Blood Flow Metab. 2012; 32:1347–1361. [PubMed: 22415525]

[67]. Jones NM, Bergeron M. Hypoxic preconditioning induces changes in HIF-1 target genes in neonatal rat brain. J. Cereb. Blood Flow Metab. 2001; 21:1105–1114. [PubMed: 11524615]

[68]. Sharp FR, Bernaudin M. HIF1 and oxygen sensing in the brain. Nat. Rev. Neurosci. 2004; 5:437–448. [PubMed: 15152194]

[69]. Helton R, Cui J, Scheel JR, Ellison JA, Ames C, Gibson C, Blouw B, Ouyang L, Dragatsis I, Zeitlin S, Johnson RS, Lipton SA, Barlow C. Brain-specific knock-out of hypoxia-inducible factor-1α reduces rather than increases hypoxic-ischemic damage. J. Neurosci. 2005; 25:4099–4107. [PubMed: 15843612]

[70]. Chen C, Hu Q, Yan J, Yang X, Shi X, Lei J, Chen L, Huang H, Han J, Zhang JH, Zhou C. Early inhibition of HIF-1α with small interfering RNA reduces ischemic-reperfused brain injury in rats. Neurobiol. Dis. 2009; 33:509–517. [PubMed: 19166937]

[71]. Chen W, Jadhav V, Tang J, Zhang JH. HIF-1 alpha inhibition ameliorates neonatal brain damage after hypoxic-ischemic injury. Acta Neurochir. Suppl. 2008; 102:395–399. [PubMed: 19388354]

[72]. Hicdonmez T, Kanter M, Tiryaki M, Parsak T, Cobanoglu S. Neuroprotective effects of N-acetylcysteine on experimental closed head trauma in rats. Neurochem. Res. 2006; 31:473–481. [PubMed: 16758355]

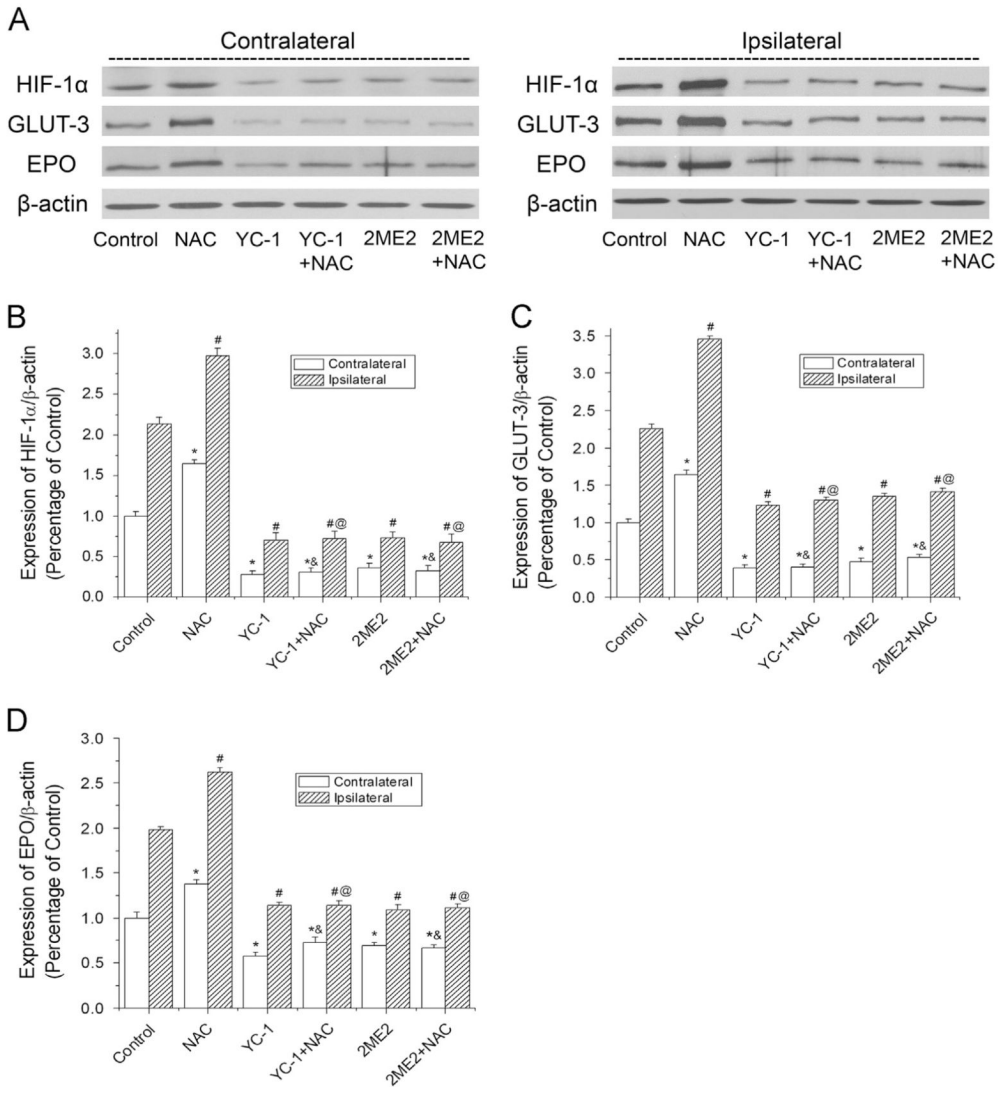


**Fig. 1.**

Effects of NAC on HIF-1α and its target gene expression in ischemic brains of rats. The protein levels of HIF-1α, GLUT-3, and EPO were analyzed by Western blotting in brain hemispheres of rats subjected to 90 min ischemia and 24 h reperfusion. Rats received NAC (150 mg/kg, ip) at 30 min before the onset of ischemia. YC-1 (2 mg/kg, iv) was administered at 24 h and 30 min before the onset of ischemia. 2ME2 (5 mg/kg, ip) was administered at 1 h before the onset of ischemia. (A) Representative Western blots of HIF-1α and its downstream proteins in contralateral and ipsilateral hemispheres. (B) Quantification of the HIF-1α protein level in contralateral and ipsilateral hemispheres. (C) Quantification of the GLUT-3 protein level in contralateral and ipsilateral hemispheres. (D) Quantification of the EPO protein level in contralateral and ipsilateral hemispheres. Values were normalized to β-actin and corresponding hemispheres of control animals. Values are means±SEM, $n$=5. *$p$<0.05 vs contralateral hemisphere from control animals. $^{\#}p$<0.05 vs ipsilateral hemisphere from control animals. $^{\&}p$<0.05 vs contralateral hemisphere from NAC animals. $^{@}p$<0.05 vs ipsilateral hemisphere from NAC animals.

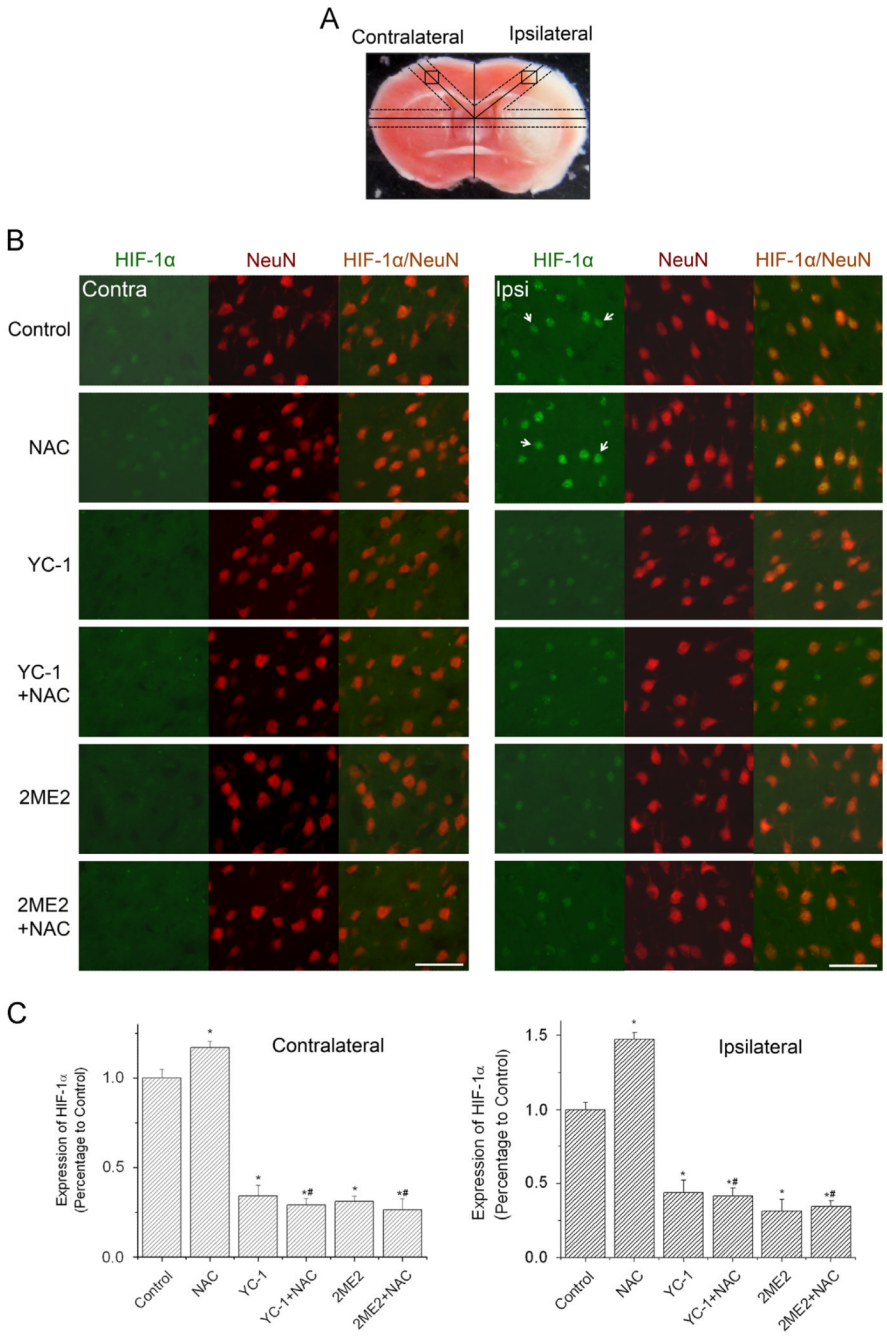


**Fig. 2.**

Effect of NAC on HIF-1 expression in neurons in ischemic brains of rats. The protein level of HIF-1α was analyzed by double immunostaining with the neuronal marker NeuN after rats were subjected to 90 min ischemia and 24 h reperfusion. Rats received NAC (150 mg/kg, ip) at 30 min before the onset of ischemia. YC-1 (2 mg/kg, iv) was administered at 24 h and 30 min before the onset of ischemia. 2ME2 (5 mg/kg, ip) was administered at 1 h before the onset of ischemia. (A) TTC-stained rat brain coronal section. Labeled square areas represent locations of immuno images (see Ref. [42] for details). (B) Double immunostaining of HIF-1α (green) and NeuN (red). The white arrows indicate positively stained neurons. Scale bar, 50 μm. (C) Quantification of the HIF-1α immunostaining

intensity in contralateral and ipsilateral hemispheres. Values are means±SEM, $n$=5. *$p$<0.05 vs control animals. $^{\#}p$<0.05 vs NAC animals. (For interpretation of the references to color in this figure legend, the reader is referred to the web version of this article.)

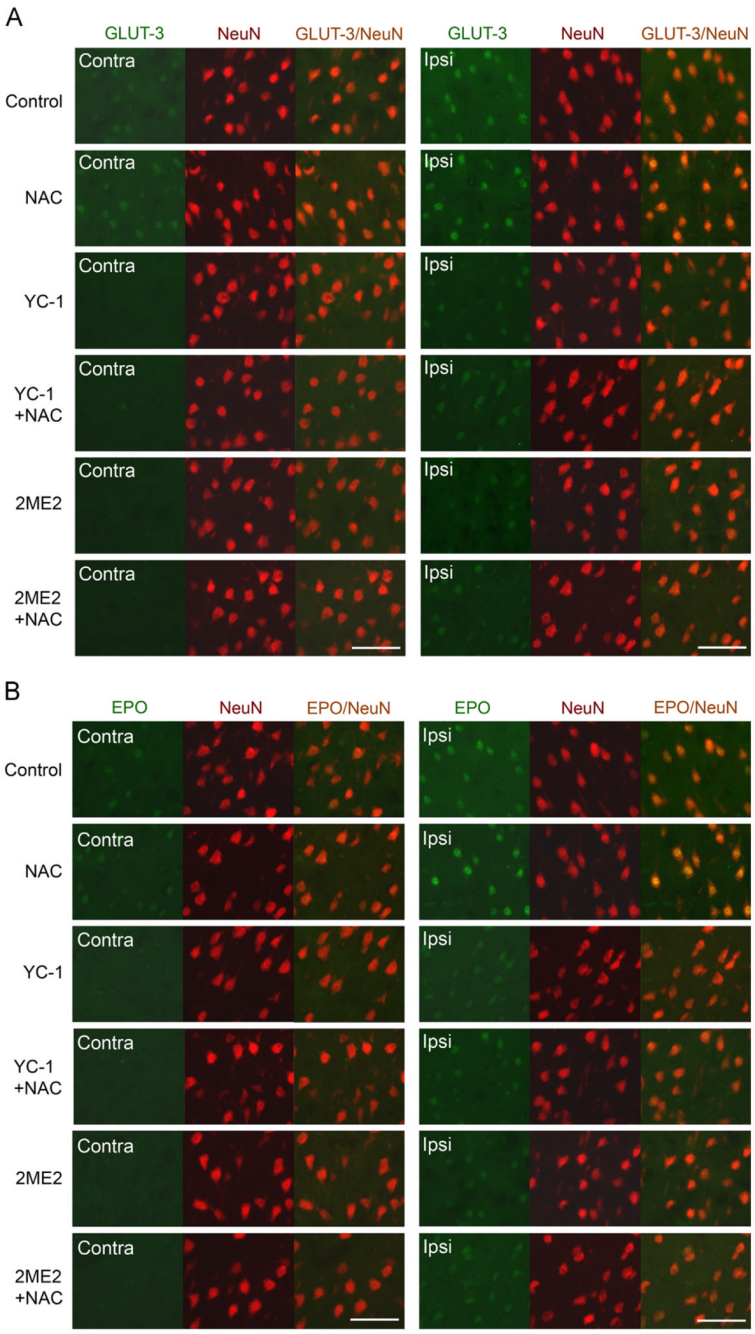


**Fig. 3.**

Effects of NAC on HIF-1 target gene expression in neurons in ischemic brains of rats. GLUT-3 and EPO were analyzed by double immunostaining with the neuronal marker NeuN after rats were subjected to 90 min ischemia and 24 h reperfusion. Rats received NAC (150 mg/kg, ip) at 30 min before the onset of ischemia. YC-1 (2 mg/kg, iv) was administered at 24 h and 30 min before the onset of ischemia. 2ME2 (5 mg/kg, ip) was administered at 1 h before the onset of ischemia. Selection of areas for imaging was the same as for those shown in Fig. 2. (A) Double immunostaining of GLUT-3 (green) and NeuN (red). (B) Double immunostaining of EPO (green) and NeuN (red). Scale bar, 50 μm. See supplementary material for statistical analyses on the images. (For interpretation of the

references to color in this figure legend, the reader is referred to the web version of this article.)

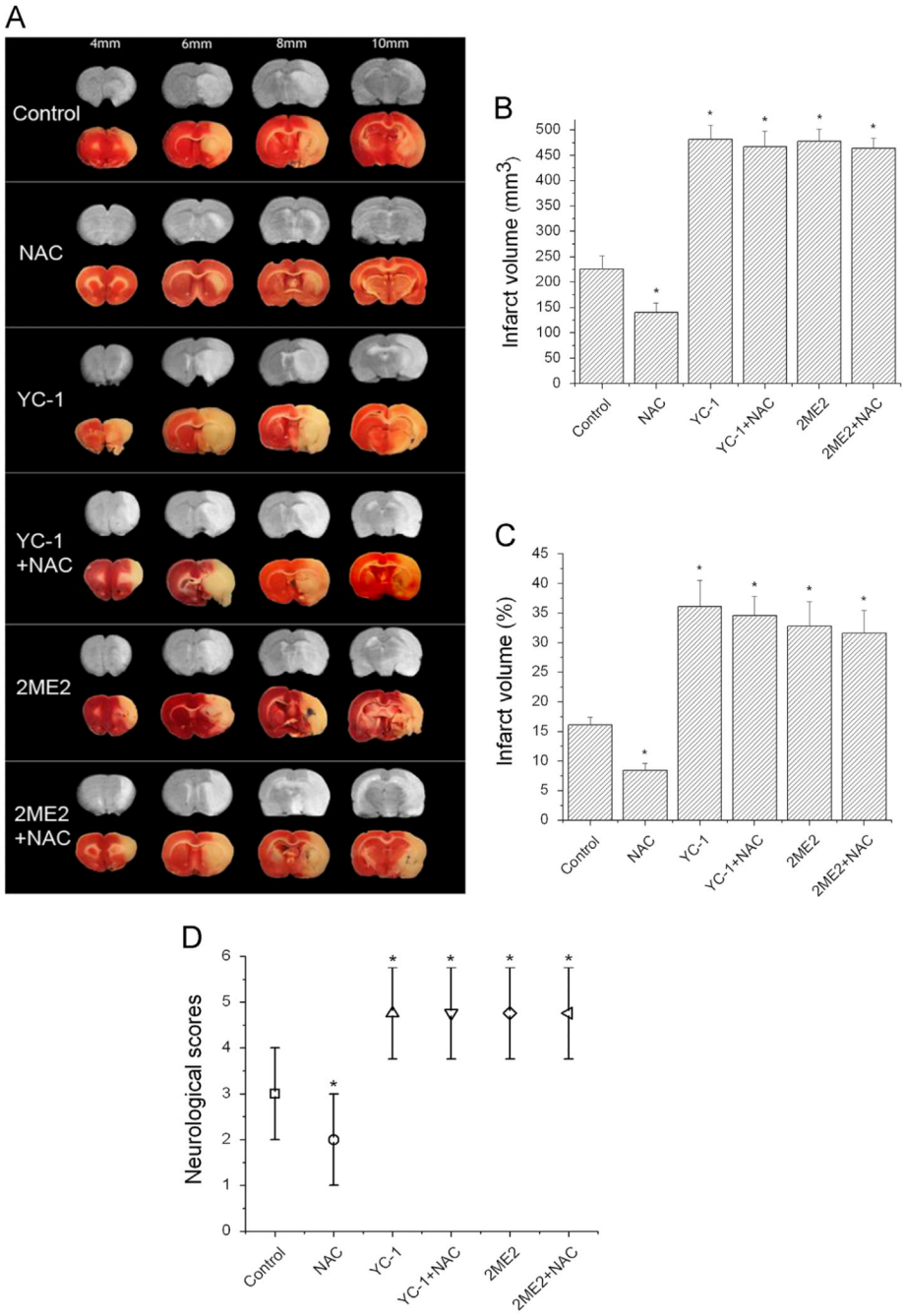


**Fig. 4.**

Effects of NAC on ischemia/reperfusion-induced brain infarction and neurological deficit. Brain infarction was estimated by MRI and TTC staining after rats were subjected to 90 min ischemia and 24 h reperfusion. Rats received NAC (150 mg/kg, ip) at 30 min before the onset of ischemia. YC-1 (2 mg/kg, iv) was administered at 24 h and 30 min before the onset of ischemia. 2ME2 (5 mg/kg, ip) was administered at 1 h before the onset of ischemia. (A) Representative TTC staining (lower rows) and T2-weighted MR (upper rows) images of MCAO brain sections of rats. The brains were sectioned beginning at the 4-mm position from the frontal pole and continued in 2-mm intervals to 10 mm. (B) Quantification of infarct volume with T2-weighted MR images of rat brain (*n*=7 (control), 8 (NAC), 5 (YC-1),

6 (YC-1+NAC), 6 (2ME2), and 7 (2ME2+NAC)). (C) Quantification of infarct volume estimated by TTC-stained sections ($n$=7 (control), 8 (NAC), 5 (YC-1), 6 (YC-1+NAC), 6 (2ME2), and 7 (2ME2+NAC)). Values are means±SEM, $^{n}p<0.05$ vs control animals. (D) Quantification of neurological deficit scores rate ($n$=22 (control), 23 (NAC), 20 (YC-1), 21 (YC-1+NAC), 21 (2ME2), and 22 (2ME2+NAC)). Values are medians with ranges, $^{n}p<0.05$ vs control animals.

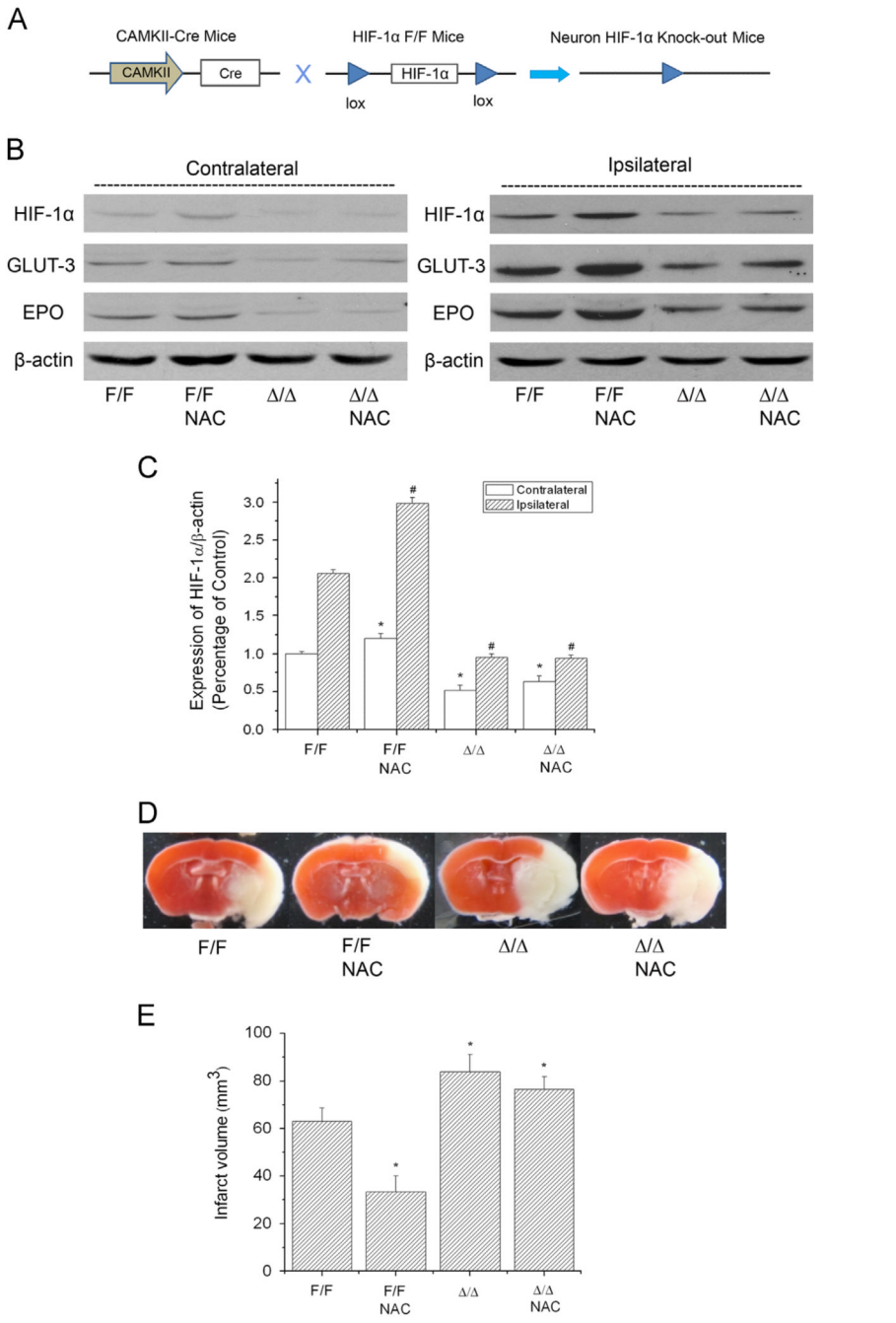


**Fig. 5.**

Effect of NAC on HIF-1 expression and ischemia/reperfusion-induced brain infarction in wild-type (HIF-1α$^{F/F}$) and neuronal HIF-1α-deficient (HIF-1α$^{\Delta/\Delta}$) mice. The protein levels of HIF-1α, GLUT-3, and EPO were analyzed by Western blotting in the brains of mice subjected to 90 min ischemia and 24 h reperfusion. Mice received NAC (240 mg/kg, ip) at 30 min before the onset of ischemia. (A) Schematic of the neuron-specific HIF-1α-knockout mouse model. (B) Representative Western blots of HIF-1α and its downstream proteins GLUT-3 and EPO. (C) Quantification of the HIF-1α protein level in contralateral and ipsilateral hemispheres ($n$=3). $^{n}p$<0.05 vs contralateral hemispheres from control (HIF-1α$^{F/F}$) mice. $^{\#}p$<0.05 vs ipsilateral hemispheres from control (HIF-1α$^{F/F}$) mice. (D)

Representative TTC staining images of brain sections of MCAO mice. The brains were sectioned from the 6-mm position from the frontal pole. (E) Quantification of infarct volume estimated from TTC-stained sections ($n$=3). Values are means±SEM, $^{n}p<0.05$ vs control (HIF-1$\alpha^{F/F}$) mice.

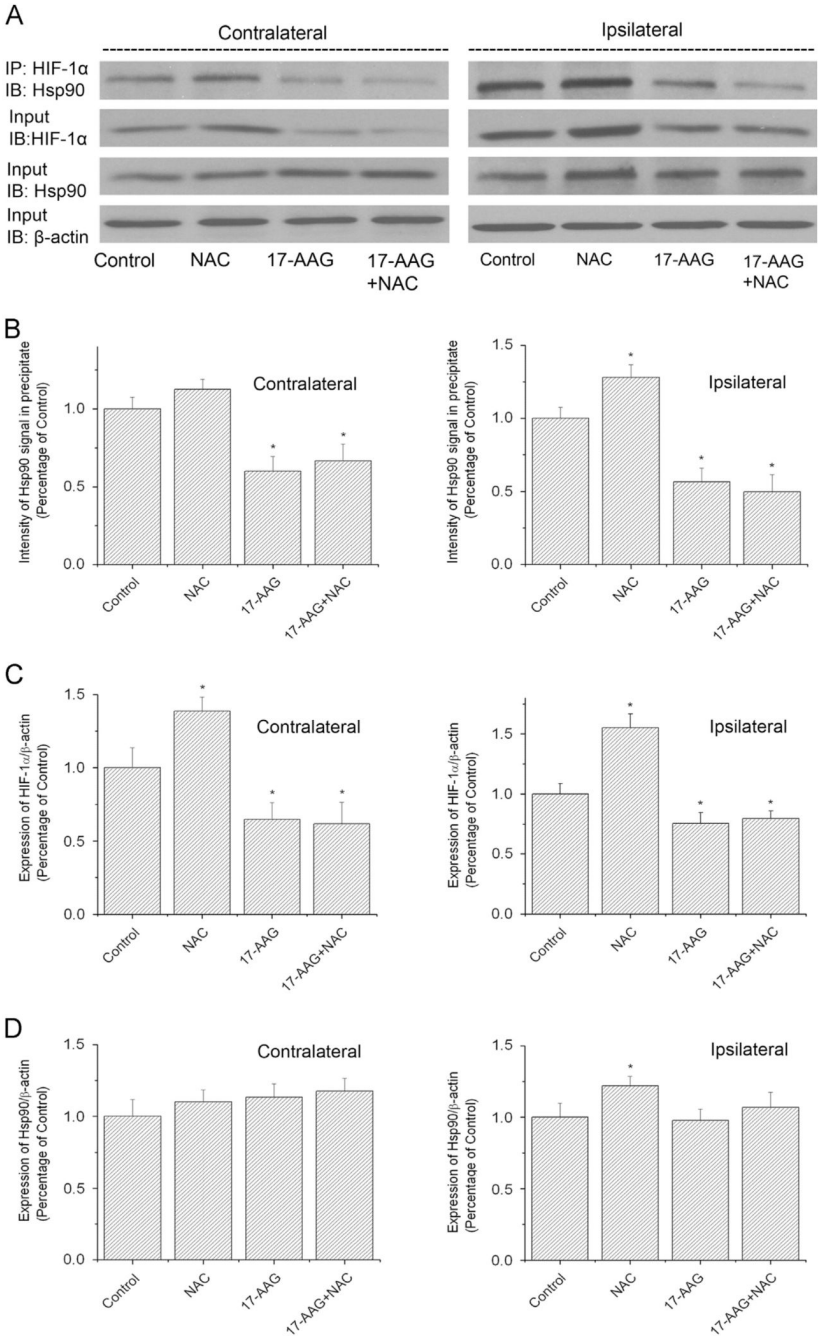


**Fig. 6.**

Effects of NAC on HIF-1α and Hsp90 interaction in ischemic brains of mice. The protein levels of HIF-1α and Hsp90 were analyzed by Western blotting in the brains of mice subjected to 90 min ischemia and 24 h reperfusion. Mice received NAC (240 mg/kg, ip) at 30 min before the onset of ischemia. 17-AAG (25 mg/kg, ip) was administered at 1 h before the onset of ischemia. (A) Representative immunoblots (IB) of HIF-1α and Hsp90 in immunoprecipitates (IP) of HIF-1α. (B) Quantification of the Hsp90 protein level in immunoprecipitates of HIF-1α in contralateral and ipsilateral hemispheres. (C) Quantification of the HIF-1α protein level in contralateral and ipsilateral hemispheres. (D) Quantification of the Hsp90 protein level in contralateral and ipsilateral hemispheres. Values

were normalized to β-actin and corresponding hemispheres of control animals. Values are means±SEM, $n=3$. $^{n}p<0.05$ vs control animals.

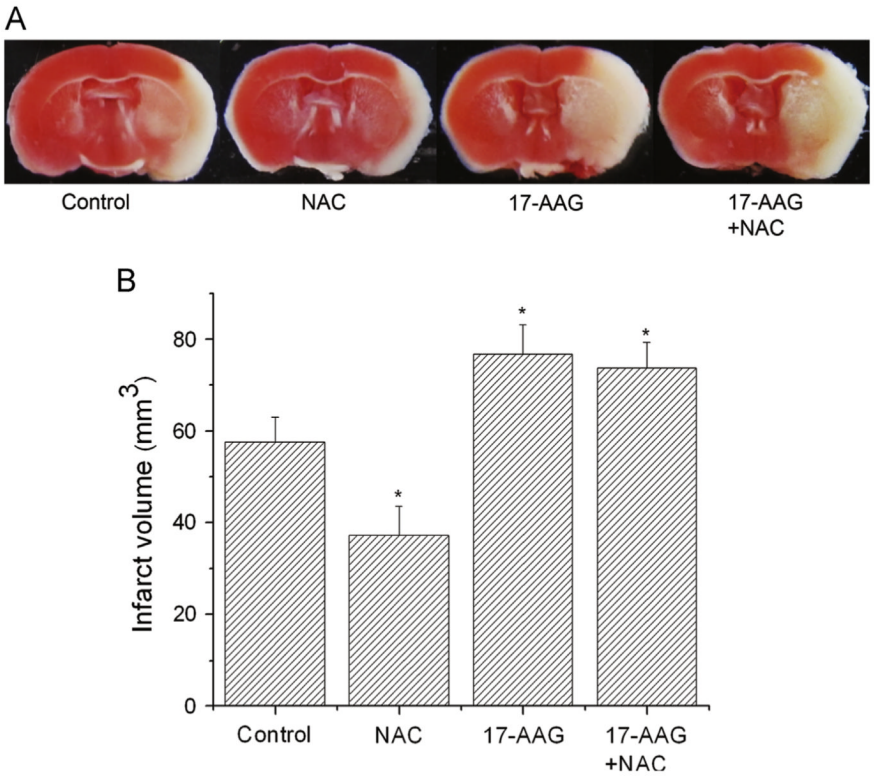


**Fig. 7.**

Effects of 17-AAG on ischemia/reperfusion-induced brain infarction in control and NAC-treated mice. (A) Representative TTC staining images of brain sections of MCAO mice. The brains were sectioned from the 6-mm position from the frontal pole. (B) Quantification of infarct volume estimated by TTC-stained sections ($n$=3). Values are means±SEM, $^{n}p<0.05$ vs control mice.

## Table 1

HIF-1α inhibitor-induced mortality of MCAO rats and groups of rats for final analyses.

| Group | Analysis | Initial group size | Failed MCAO[a] | Death after successful MCAO[b] | Group size for final analysis |
|---|---|---|---|---|---|
| MCAO | MRI+TTC | 7 | 0 | 0 | 7 |
| MCAO | HIF | 18 | 1 | 2 | 15 |
| MCAO | Total | 25 | 1 | 2 (8.3%) | |
| NAC | MRI+TTC | 10 | 1 | 1 | 8 |
| NAC | HIF | 15 | 0 | 0 | 15 |
| NAC | Total | 25 | 1 | 1 (4.2%) | |
| YC-1 | MRI+TTC | 10 | 1 | 4 | 5 |
| YC-1 | HIF | 20 | 1 | 4 | 15 |
| YC-1 | Total | 30 | 2 | 8 (28.6%) | |
| YC-1+NAC | MRI+TTC | 10 | 1 | 3 | 6 |
| YC-1+NAC | HIF | 20 | 1 | 4 | 15 |
| YC-1+NAC | Total | 30 | 2 | 7 (25.0%) | |
| 2ME2 | MRI+TTC | 11 | 0 | 5 | 6 |
| 2ME2 | HIF | 19 | 1 | 3 | 15 |
| 2ME2 | Total | 30 | 1 | 8 (27.6%) | |
| 2ME2+NAC | MRI+TTC | 10 | 0 | 3 | 7 |
| 2ME2+NAC | HIF | 20 | 1 | 4 | 15 |
| 2ME2+NAC | Total | 30 | 1 | 7 (24.1%) | |

[a]Failed MCAO: animals were excluded because of a lack of obvious neurological deficit, which occurred when the suture was not placed at the right location to block the middle cerebral artery (MCA).

[b]Death after successful MCAO: occlusion of the MCA was successful but the animal died primarily because of intracranial bleeding during the procedure. The intracranial bleeds happened when the monofilament suture was inserted too far and perforated the anterior cerebral artery. When the bleed occurred, the animal died from bleeding within the first 2 h postreperfusion. For all the animals used for final analyses, no signs of hemorrhage were observed.